

University of Sheffield

Patient-specific modelling of intracranial aneurysm evolution



Yifan Pu

Supervisor: Dr. Paul Watton

A report submitted in fulfilment of the requirements
for the degree of MSc in Advanced Computer Science

in the

Department of Computer Science

September 8, 2017

Declaration

All sentences or passages quoted in this report from other people's work have been specifically acknowledged by clear cross-referencing to author, work and page(s). Any illustrations that are not the work of the author of this report have been used with the explicit permission of the originator and are specifically acknowledged. I understand that failure to do this amounts to plagiarism and will be considered grounds for failure in this project and the degree examination as a whole.

Name:

Signature:

Date:

Acknowledge

I would begin by thanking my supervisor, Dr. Paul Watton for helping me solve lots of problems through his busy schedules. This has played a major role in my successful completion of the project.

Then, I would thank Yuqian Mei, a doctoral student of Dr. Paul Watton. Yuqian has been like my second supervisor. Because my major is not related to the biomechanics and I do not have any background about the aneurysm, Yuqian helps me know a wide range of basic knowledge and correct me where wrong. In addition, she shows me the right direction to proceed. I am extremely grateful for all support she has given me.

Also, I would like to thank all my professors who had taught me. Under your patient guidance, I have learnt so much useful knowledge, which is important for my future career and life.

Lastly, I will thank my friends met in Sheffield. It is you who made my life of studying aboard so colourful.

Abstract

This dissertation introduces a new approach to model the patient-specific modelling of intracranial aneurysm evolution, which can be used in some further applications. Compared with standard aneurysm modelling method, this project could build any three-dimensional model, which could fit the patient-specific demand better. Because different aneurysms have their own shapes, the calculation algorithm about curvature direction of their surface geometry is applied to analyse the fiber orientation conditions of these aneurysm. The strain energy function put forward by professor Holzapfel is used to realize the growth modelling of aneurysm. In terms of some special changing material parameters about the collagen remodelling, such as k_2 , in this modelling process, a new equation is introduced to measure these values for the next modelling step. In the end of this dissertation, some figures about the modelling results will be demonstrated.

Key Words: modelling, curvature, strain energy function

Contents

1	Introduction	1
1.1	Intracranial Aneurysm	1
1.2	Diagnosis and Treatment	2
1.3	Reason For Study/Motivation	4
1.4	Overview of Report	4
2	Literature Survey	6
2.1	Pathophysiology	6
2.1.1	The Structure of Blood Vessel	6
2.1.2	Role of Endothelial Cells in the Aneurysms Evolution	7
2.1.3	Growth and Remodelling of Collagen Fibers	8
2.1.4	Elastin Degradation	9
2.2	The Model of the Remodelling of Aneurysm	9
2.2.1	The Holzapfel Model—Multi-layer Model for Arterial Walls . .	9
2.3	The Relationship between Aneurysm Geometry and Growth	12
3	Requirements and Analysis	14
3.1	Mathematical Foundations	14
3.1.1	The Calculation of Principal Curvature Direction	14
3.1.2	Interpolation	17
3.1.3	Euclidean Distance	18
3.2	Analysis	20
3.2.1	Improvements	20
3.2.2	Limitations	20
4	Implementation	22
4.1	The Prepare of Modelling Aneurysm Evolution	22

4.1.1	The Establishment of the Aneurysm Model	22
4.1.2	Analysis of Principal Curvature of Aneurysm Geometry	24
4.1.3	Determination of the Initial Parameters	25
4.1.4	The Boundary Condition	26
4.2	The Modelling Loop of the Growth Process of Aneurysm	27
4.2.1	Overview of Whole Progress	27
4.2.2	Handling the Parameter by Utilizing Holzapfel Model	27
4.2.3	The Algorithm to Deal With the Output Stress Results	29
4.2.4	Region Control	29
5	Results and Discussions	32
5.1	The Results about Pintcipal Curvature Direction of Different Aneurysms	32
5.2	Data Processing Progress	32
5.3	The Modelling of Aneurysm Evolution about Whole Geometry	34
5.4	The Modelling of Aneurysm Evolution about the Localization Part .	37
6	Conclusion	39
6.1	Conclusion	39
6.2	Limitations	40
7	Future Work	41

List of Figures

1.1	Endovascular Occlusion with the Utilization of Detachable Coils(coiling)[1]	3
1.2	Craniotomy with Clip Ligation (clipping)[1]	3
2.1	The Structure of the Blood Vessel[2]	7
2.2	The Structure of the Artery and the Main Cell Types Involved in Endotheliocyte Growth [3]	8
3.1	Saddle Surface with Normal Planes in Directions of Principal Curvatures[4]	15
3.2	Local Orthogonal Coordinate System[5]	16
3.3	Euclidean Distance(2D)[6]	19
3.4	Euclidean Distance(3D)[7]	19
4.1	Preprocessing Part of Remodelling	23
4.2	Standard Tetrahedron and Tetrahedron with Intermediate Points	24
4.3	The Meshing Result	24
4.4	The Distribution of Principal Curvature(1st and 2nd) Direction of new Aneurysm model. (In addition, the red vector is the 1st principal direction and the blue vector is the 2nd principal direction)	25
4.5	Ansys Input Format[8]	26
4.6	The Flow Chart of Remodelling Progress	28
4.7	The Distribution of Different Value of the Related Material Oarameters(c) in the Aneurysm Model	30
4.8	The Process of How the Related Material Parameters Change	31
5.1	The Distribution of Principal Curvature(1st and 2nd) Direction of Aneurysm(1)	33
5.2	The Distribution of Principal Curvature(1st and 2nd) Direction of Aneurysm(2)	33

5.3	The Distribution of Principal Curvature(1st and 2nd) Direction of Aneurysm(3)	34
5.4	The Flow Chart of Remodelling Progress	35
5.5	Modelling of Aneurysm Whole Geometry Evolution	36
5.6	Modelling of Aneurysm Localization Evolution	37

List of Tables

5.1	The DMX in Different Parameters	35
5.2	The Change of Shear Modulus (c) of the Localization Domain	38

Chapter 1

Introduction

1.1 Intracranial Aneurysm

Aneurysm is a kind of saccular bulge in the artery, which caused by the local expansion of the arterial wall. Generally, the formation of aneurysm is more common in the region of brain and this category of aneurysm is named intracranial aneurysm (also called cerebral or brain aneurysm) [2]. An intracranial aneurysm grows on the wall of an artery, leading to the bulging of this arterial wall's region. It means that this region of artery will swell, like a balloon. In addition, the wall will become weak and thin in the progressing course of bulging. As a result, there is a danger that the intracranial aneurysm will rupture and it will result in the brain bleeding—subarachnoid hemorrhage[1].

Intracranial aneurysms is a relatively common disease due to its high morbidity about 1 to 5 percent of adults[1]. However, the intracranial aneurysms, under most cases, are relatively small and 50 to 80 percent of aneurysms will not rupture during the whole life of one person [1].

There are two main types of aneurysms, saccular aneurysm and fusiform aneurysm. Saccular aneurysm, which is like the shape of berry, is the most common form of intracranial aneurysm. In addition, this kind of aneurysm is broadly found along the Circle of Willis[2].

Compared with that of saccular aneurysm, the shape and the forming place of fusiform aneurysm are extremely different. Fusiform aneurysm affects more regions of the blood vessel, it means that when the fusiform aneurysm occurs, the whole vessel section will extend instead of bulging just in one side of the arterial wall. Also, Fusiform aneurysm can be ordinarily found in the belly main artery and popliteal aorta behind the knee[2].

1.2 Diagnosis and Treatment

Intracranial aneurysm is a sort of extremely dangerous disease. The person who has the intracranial aneurysm has not any special symptom unless when the intracranial aneurysm ruptures [1]. It is assessed that nearly 5%-15% stroke cases are connected with the ruptured intracranial aneurysm and the occurring rate of subarachnoid hemorrhage among people carrying intracranial aneurysm is about 1:1000 in America [1]. The subarachnoid hemorrhage is a form of hemorrhagic stroke with high mortality. Even these people can survive, approximately 30% of them will get serious disability.

There are three main approaches to make sure or fix the location of intracranial aneurysm. They are CT angiography, magnetic resonance angiography and direct intra-arterial catheterization. It is acknowledged that the last one is the standard method in this domain.

After locating the intracranial aneurysm, the next step is to treat this disease. Two curing choices are providedcraniotomy with clip ligation (clipping)(Fig 1.2), and endovascular occlusion with the utilization of detachable coils(coiling)(Fig 1.1).

The first treating way is to access the aneurysm by using craniotomy and then clip some steady material on the neck of aneurysm to ligate; the other way is to occlude the aneurysm with coils through a micro catheter inserted from other body part. Overall, these two treating options are not perfect approaches because they both have their own disadvantages. The main risk of clipping is incomplete occlusion, whereas that of the other is thromboembolic phenomena.

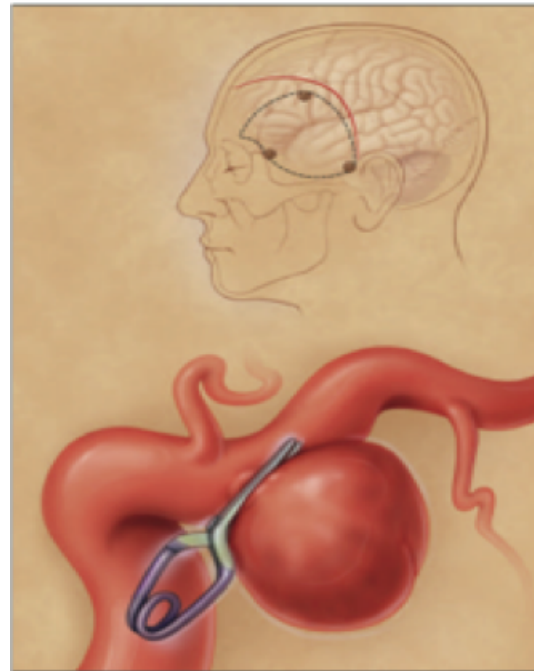


Figure 1.1: Endovascular Occlusion with the Utilization of Detachable Coils(coiling)[1]

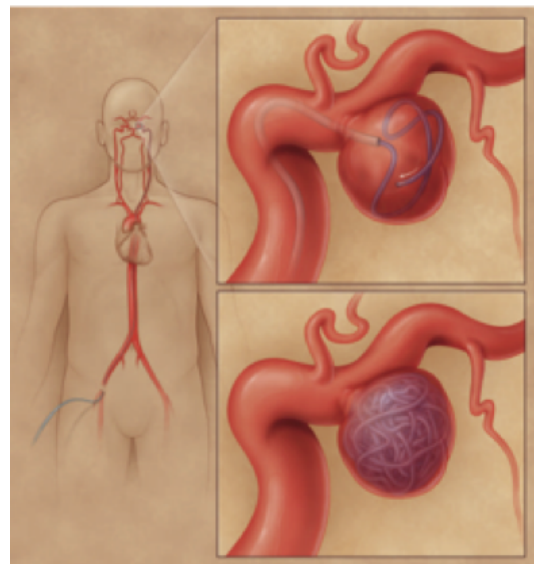


Figure 1.2: Craniotomy with Clip Ligation (clipping)[1]

1.3 Reason For Study/Motivation

The aim of this research is to find out a new method to analyse the surface of intracranial aneurysm, which can help to remodel the growth progress of aneurysm better. The fundamental analytic approach is to utilize Neo-Hookean model. This is a model based on the Hooke's law[9]. However, in terms of Neo-Hookean model, it only takes the influence of stress on strain (which will be discussed further in the chapter below) into consideration. So, a new model was established by professor Holzapfe[10]. Holzapfer brought forward a new option about the influence of stress on the arterial tissue. In some past related research, Holzapfel's model was usually used to analyse the behaviours of arterial walls[11][12]. Because the blood vessels can be meshed into a wide range of structured grids and it will be easily to analyse each element in the vessels[13]. In order to analyse any 3D aneurysm model, the adoption of the Neo-Hookean model is far from fitting the patient-specific demand. In this paper, the model established by Holzapfel [10] will be used to solve some problems about anisotropic hyperelasticity collagen remodelling. Given that the irregular surface of aneurysm, it is difficult to build the standard structured grids. The unstructured grids are used to mesh the patient-specific aneurysm. To these grids, some specific element parameters are added to model the growth of aneurysm. In addition, in allusion to any domain of aneurysm, the degree of elastin degradation can be observed.

1.4 Overview of Report

In the Chapter 2, some information that related to this project in the previous papers will be introduced, including the alteration of collagen and elastin in the formation and growth of aneurysm and the model of remodelling of aneurysm utilized in this project.

Turing to the Chapter 3, during the design resolutions of this project, there are some mathematics foundations associated with the analysis process should be explained further.

In the Chapter 4, the whole implementation of modelling process will be detailed. The modelling process will be divided into two part: the pretreatment of the aneurysm model and the simulation process of aneurysm growth in different time period.

In the Chapter 5, it will be illustrated about the modelling results, such as some figures and tables. In addition, the variance of material parameters will be described in some particular time periods.

In the Chapter 6, it mainly demonstrates some conclusions achieved from this project. Some limitations definitely exist in this project, which will be listed as well.

In the Chapter 7, on the basis of the limitations listed in the last chapter, some solutions will be analysed. These solutions are just preliminary ideas which should be improved in the future work.

Chapter 2

Literature Survey

2.1 Pathophysiology

2.1.1 The Structure of Blood Vessel

The structure of blood vessels in humans body is demonstrated in the picture below(Fig 2.1). The blood vessel is consisted of three layers: tunica external (adventitia), tunica media (or muscle) and tunica intima. The outermost layer is tunica adventitia. This layer is made up of ground substances, collagen fibers, vasa vasorum that supply the blood vessel, and nerves that extend into the interlayer [2]. Turning to the tunica media layer which is considered as the median blood vessels layer, it is almost twice thicker than the adventitia [14]. The main compositions of this layer are smooth muscle cells, some supporting and connecting elastic sheets as well as collagenous fibers. The flexibility of the vessel wall is regulated by this layer via its segments such as smooth muscle cells. It means that the tunica media layer controls the mechanical attributes of vessel wall.

The deepest layer is the tunica intima. The structure of tunica intima is simpler than the other two layers. It is consisted of basement membrane and vascular endothelial cells which attach to a basal lamina. The hidden part behind basal lamina is a sub-endothelial layer made up of some elastic and collagenous ingredients.

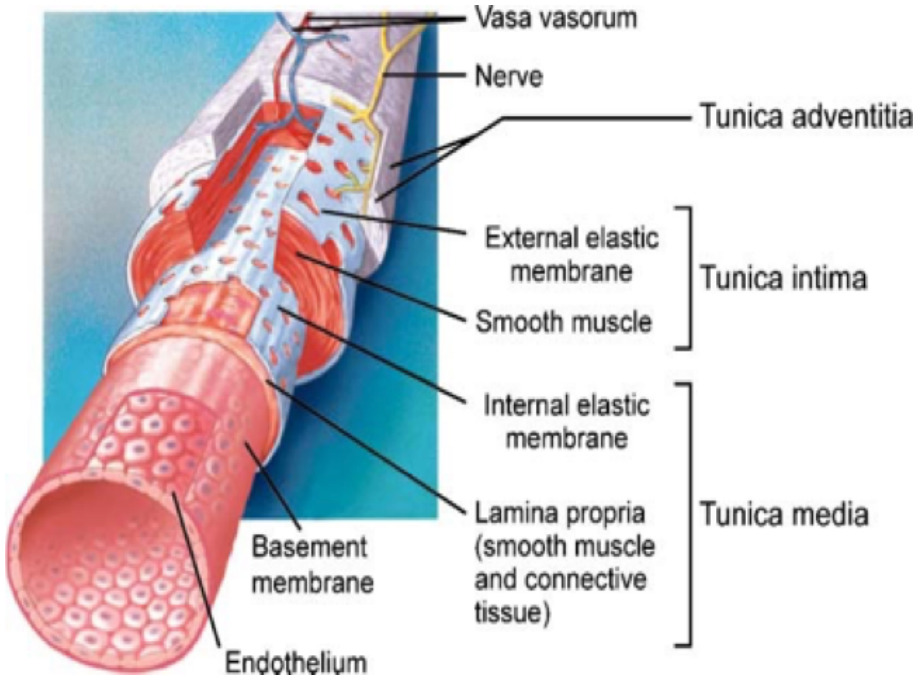


Figure 2.1: The Structure of the Blood Vessel[2]

2.1.2 Role of Endothelial Cells in the Aneurysms Evolution

Vascular endothelial cells (ECs) adjust their morphology during the hemodynamic circle and affect the structure and function of the artery walls. A basement membrane covering a single layer of endothelial cells consists the intima. The margin edge of these endothelial cells is not smooth in order to connect to others. The main function of endothelial cells is to adjust the influence of the haemodynamic forces on the article wall and act as a boundary separating blood flow [15]. In addition, endothelial cells are in the place between plasma and vascular tissue and they can not only achieve the cellular substance (supply nutrients, growth factors and oxygen) exchange, but also produce some biochemical signals. Because the main framework of endothelial cell is made up of three polymers: microtubules, intermediate filaments, and F-actin. The last component F-actin controls a wide range of protein and these protein will be arranged and managed for stability, flexibility and force formation[16]. These functions can help to keep the healthy hemodynamic environment.

However, due to the highly dynamic blood flow pulsatility, some problems(such as the variation of some mechanical stresses)will easily occur in the original hemodynamic

environment. Vast alterations on cytoskeleton and morphology will result in cellular elongation and alignment in the direction of blood flow. This means that the endothelial cells are sensitive to temporal shear gradients and spatial shear gradients

2.1.3 Growth and Remodelling of Collagen Fibers

Collagen protein is a kind of skeleton structure of extracellular matrix, while elastin is an important structure of blood vessel and plays an important role in maintaining the elasticity and bionomics of the blood vessel. This extracellular matrix plays an important role in endotheliocyte growth and tissue regeneration (Fig 2.2).

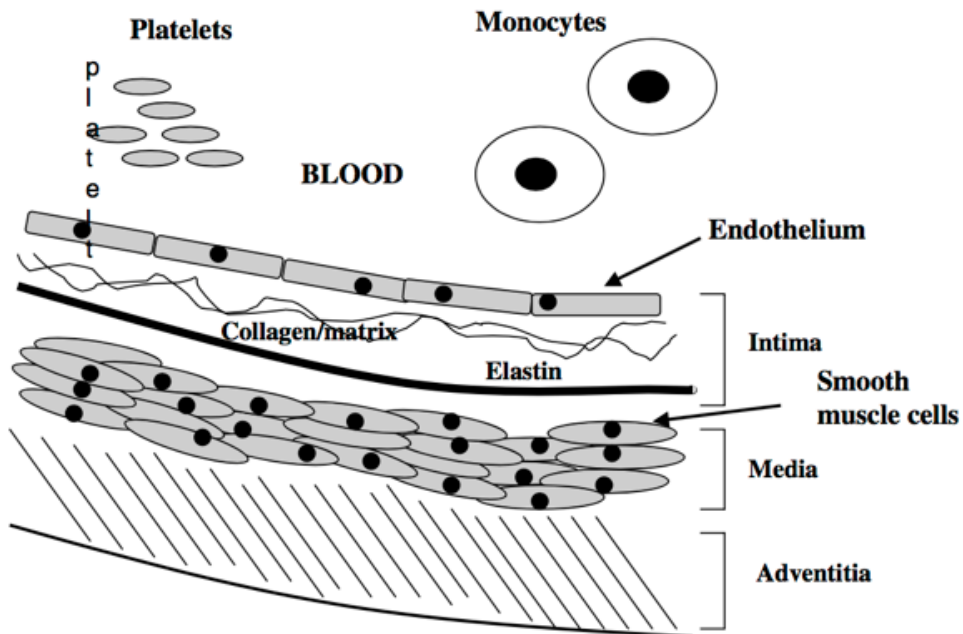


Figure 2.2: The Structure of the Artery and the Main Cell Types Involved in Endotheliocyte Growth [3]

In order to achieve a new blood vessel environment balance and reduce the influence conducted by the degradation of elastin, the collagen fibers constantly remodel to bear load. The adaptive response of collagen fabric includes growth and remodeling.

In healthy artery, the number of collagen fibers keeps steady because of continual proliferation and degradation. However, due to some changes in the vessel environment, vessel cells will adjust by up-regulating synthesis and down-regulating degradation[15].

The growth of collagen fiber is associated with the evolving of fiber concentration. At the same time, fibroblast will be affected by this increasing. There is a development of collagen synthesis and a decreasing about enzymes which diminish the growth of collagenous matrix[14]. Considering the other aspect—remodeling, collagen fibers will accomplish the maximum stretch in the blood flow circle.

2.1.4 Elastin Degradation

The essential cause of the aneurysm formation is the degradation of elastin, which will lead to a confusion in the arterial geometry. In terms of the structure, at the neck region, a saccular intracranial aneurysm causes because of an unexpected damage of the media layer within the dome patch[15]. To capture the damage of the media layer, the elastin fibers circularly degrade in the center of a domain which leading to a confusion to the blood flow environment. In turn, the distribution of wall shear stress (WSS) will be influenced[15].

2.2 The Model of the Remodelling of Aneurysm

2.2.1 The Holzapfel Model—Multi-layer Model for Arterial Walls

In the multi-layer model, the artery is made up by three layers. In order to simplify model, the materials in each layer can be reduced to the combination of two families of fibres which are arranged in symmetrical spirals and similar mechanical characteristics[10]. Also, a similar each layer pattern of strain-energy function [17] can be adopted in each layer. The result $\bar{\Psi}$ from the strain-energy function can be divided into two different parts: $\bar{\Psi}_{iso}$ and $\bar{\Psi}_{aniso}$. $\bar{\Psi}_{iso}$ represents isotropic deformation and $\bar{\Psi}_{aniso}$ means anisotropic deformation [10].

In terms of $\bar{\Psi}_{iso}$, it is supposed to be related to mechanical response of the non-collagenous. Under low pressure, the collagen fibers will not store energy. By contrast, under high pressure, collagen fibers is responsible for the resistance to stretch. It means that $\bar{\Psi}_{aniso}$ is associated with the mechanical response of collagenous matrix material. The equation below is the full strain-energy formula[10].

$$\bar{\Psi}(\bar{C}, a_{01}, a_{02}) = \bar{\Psi}_{iso}(\bar{C}) + \bar{\Psi}_{aniso}(\bar{C}, a_{01}, a_{02}) \quad (2.1)$$

As mentioned before, each artery layer consists of families of collagenous fibers and $\bar{\Psi}_{aniso}$ is connected with collagenous materials. This is the parameters about collagenous fibers(a_{01}, a_{02} , their value: $|a_{0i}| = 1$) need to be added in the formula. The a_{01}, a_{02} are blended as A_i ($i = 1, 2$) by $a_{01} \otimes a_{02}$.

The value of \bar{I}_3 is a constant and there is no parameter about \bar{C} in the parameter list of \bar{I}_9 . This means that \bar{I}_3 and \bar{I}_9 will not affect the the whole function. Hence, the function(2.1) can be simplified to the function below[10].

$$\begin{aligned} \bar{\Psi}(\bar{C}, A_1, A_2) = & \bar{\Psi}_{iso}(\bar{I}_1, \bar{I}_2) + \\ & \bar{\Psi}_{aniso}(\bar{I}_1, \bar{I}_2, \bar{I}_4, \dots, \bar{I}_8) \end{aligned} \quad (2.2)$$

The formula (2.2) can be simplified to equation (2.3) further. Turning to the \bar{I}_4 and \bar{I}_6 , this two invariants has their own physical meanings. They are stretch parts for the two families of collagen fibers because the directions of \bar{I}_4 and \bar{I}_6 follow the directions of a_{01} and a_{02} , respectively. And their values are the square of stretches following their own direction. In addition, the characteristic of anisotropy is determined by \bar{I}_4 and \bar{I}_6 [10].

$$\bar{\Psi}(\bar{C}, A_1, A_2) = \bar{\Psi}_{iso}(\bar{I}_1) + \bar{\Psi}_{aniso}(\bar{I}_4, \bar{I}_6) \quad (2.3)$$

Turning to the first part of the right the right-hand side of equation (eq:2.3), $\bar{\Psi}_{iso} (\bar{I}_1)$ has been described from the Neo-Hookean model. The Neo-Hookean model is a kind of hyperelastic material model. This model is always adapted to describe the behaviour of materials about stress-strain[18]. It is obvious that the Neo-Hookean model follows the Hooke's law. Under some deformations, the stress-strain curve will become fluctuating. This means that at first, the relation between stress and strain is linear, however, in some peculiar point, this curve will maintain the non-linear state.

The equation below is the strain energy density function for an incompressible Neo-Hookean material[18].

$$I_1 = \lambda_1^2 + \lambda_2^2 + \lambda_3^2 \quad (2.4)$$

I_1 is the first invariant of the left Cauchy-Green deformation tensor[9], and the λ_i represents the principal stretches.

The Neo-Hookean model does not suitable to calculate the deformation of material at large strains. Although this model is capable to be applied on the rubber-like materials to predict initial linear range because the phenomenon that the statistical thermodynamics of cross-lined polymer chains forms the foundation of the Neo-Hookean model[9]. When the stress-strain curve get to a certain point, a dramatic increase will occur in the elastic modulus of the material[9].

The $\bar{\Psi}_{iso}$ can be explained by the Neo-Hookean model, and the classic parameter C_1 is changed to $\frac{c}{2}$. c is a stress-like material parameter and the value is always greater than 0[10]. Hence, the formula of the isotropy part is the equation below:

$$\begin{aligned} \bar{\Psi}_{iso} &= (\lambda_1^2 + \lambda_2^2 + \lambda_3^2) \\ &= \frac{m^E c}{2} (\lambda_1^2 + \lambda_2^2 + \lambda_3^2 - 3) \end{aligned} \quad (2.5)$$

where m^E represents the evolution of the elastin concentration [14].

The next part is the expression for the anisotropy. As mentioned before,in the high pressure environment,the resistance to stretch is nearly caused by collagen fibers. Due to this kind of setting, the strain energy stored in the collagen fibers is assumed to increase with an exponentially growing number. Hence, the mathematical expression of the stretch is like the equation below[10] :

$$\overline{\Psi}_{iso}(\bar{I}_4, \bar{I}_6) = \frac{m^C k_1}{2k_2} \sum_{i=4,6} \{ \exp[k_2(\bar{I}_i - 1)^2] - 1 \} \quad (2.6)$$

In the equation (2.6), k_1 and k_2 stand for a stress-like material parameter and a dimensionless parameter, respectively. On top of this, their values are always greater than zero. The collection of optimum value of k_1 and k_2 is of importance because it will greatly affect the validity of the hypothesis that the artery's mechanical characteristic will not be influenced to be modelled by collagenous fibers in the low pressure realm[19]. And m^C represents average collagen concentration [14].

Combining the equation(2.2) with the equation(2.3), the final expression of Cauchy stress tensor $\overline{\Psi}$ can be received.

2.3 The Relationship between Aneurysm Geometry and Growth

The research aim of this paper is to model the progress of patient-specific aneurysm evolution. In consideration that fiber reorientation (elastin degradation and collagen reorientation) plays a significant role in the aneurysm evolution and the surface geometry of patient-specific aneurysm is irregular, it is essential to understand the relationship between aneurysm's geometry and fiber reorientation.

Professor Baoshun Ma presented a view that the local material fiber directions are likely related to surface curvature for stable aneurysms[20]. In the paper, in terms of an axisymmetric membrane, the stress resultants tension in the meridional (local 1)

and circumferential (local 2) directions, under internal pressure P , can be indicated in the formulas below[20].

$$T_1 = \frac{P}{2k_2} \quad (2.7)$$

$$T_2 = \frac{P}{k_2} \left(1 - \frac{k_1}{2k_2}\right) \quad (2.8)$$

In the equations (2.7)(2.8), k_1 and k_2 are local principal curvatures for the meridional and circumferential directions, respectively. This means that the local surface geometry can affect the value of stresses and the principal stress directions are related with principal curvature directions[20].

Linking the theory above with the standpoint, effective collagen fiber direction at a given point on the aneurismal surface is largely dependent on local stress[21], raised by Wayne Carver et al. in 1991, we can research through the local aneurysm geometry to figure out the fiber reorientation and remodel the evolution of aneurysm.

Chapter 3

Requirements and Analysis

3.1 Mathematical Foundations

3.1.1 The Calculation of Principal Curvature Direction

The principal curvature consists of two parts: the maximum value and the minimum value of whole curvatures. In the three-dimensional Euclidean space, for each point p of a differentiable surface, a unit normal vector(Fig. 3.1) can be picked and it will be involved in a normal plane at p . In addition, normal section, an extraordinary direction tangent(Fig. 3.1) to the surface and cut the surface in a plane curve, will be involved in this normal plane[22]. The plane curve(Fig. 3.1) will have a wide range of curvatures for different normal planes at p . Among these curvatures, the maximum value k_1 and the minimum value k_2 of curvatures are selected as the principal curvature[22].

In 1760, Euler draw an conclusion that the direction of the principal curvatures (k_1 and k_2) are always perpendicular ,if k_1 does not equal k_2 [22]. This is also called principal directions. Gaussian curvature K is defined as the product $k_1 \cdot k_2$ of the two principal curvatures, turning to that of mean curvature H , it is the average $(k_1 + k_2)/2$. If at least one of the principal curvatures is zero at every point, the Gaussian curvature will be 0. For a minimal surface, the mean curvature is 0 at every point [23].

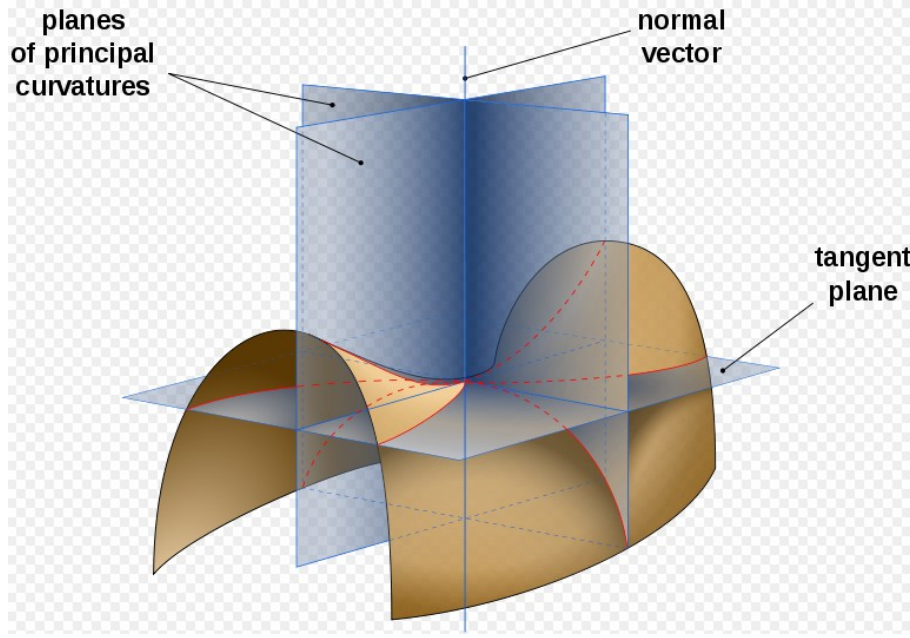


Figure 3.1: Saddle Surface with Normal Planes in Directions of Principal Curvatures[4]

Here is solution of the calculation of k_1 and k_2 , including their values and directions. Take the node p on the surface, we should build a local orthogonal coordinate system (X_1, X_2, N) . In this coordinate system(Fig. 3.2), at the node p , X_1 and X_2 are unit vectors in the tangent plane and N is the unit normal vector. The next step is to determine the weighted average of unit normals of all adjoining elements (those elements adjacent to node p), with the element areas as the weights [24]. In the local coordinate system, a bivariate polynomial $f(u, v)$ of degree two (Eq:3.1)is utilized to suggest a quadratic surface path combining the node p with its neighbour nodes.

$$f(u, v) = au^2 + buv + cv^2 \quad (3.1)$$

In terms of this surface patch, the Gauss-Weingarten map[24] can be built:

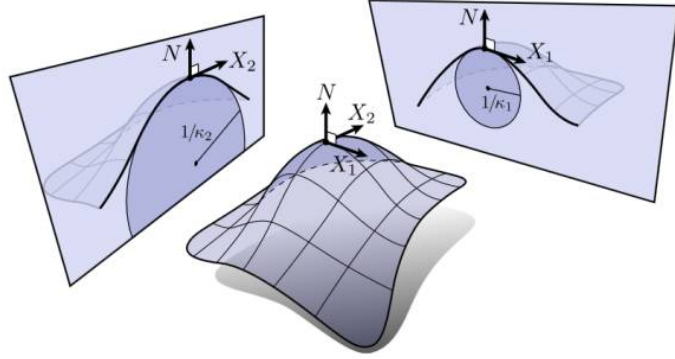


Figure 3.2: Local Orthogonal Coordinate System[5]

$$A = \begin{pmatrix} 2a & 2b \\ 2b & 2c \end{pmatrix} \quad (3.2)$$

According to the matrix A (eq:3.2), the eigenvalues (k_1 and k_2) and eigenvectors(v_{10} and v_{20}) can be calculated. Eigenvalues and eigenvectors represent the principal curvatures and principal directions[24], respectively. The expressing formula of the two parameters are like:

$$k_1 = a + c + \sqrt{(a - c)^2 + 4b^2} \quad (3.3)$$

$$k_2 = a + c - \sqrt{(a - c)^2 + 4b^2} \quad (3.4)$$

$$v_{10} = (2b, a - c + \sqrt{(a - c)^2 + 4b^2}) \quad (3.5)$$

$$v_{20} = (2b, a - c - \sqrt{(a - c)^2 + 4b^2}) \quad (3.6)$$

The v_{10} and v_{20} also need to be normalized. Note that all the calculation is based on the local coordinate system(X_1, X_2, N), it means that the principal direction is only suitable for the node p and its directly connected nodes. The following step

is to transfer v_{10} and v_{20} from the local coordinate system to the global coordinate system[24].

$$V_j = \begin{pmatrix} (X_1)_x & (X_2)_x & N_x \\ (X_1)_y & (X_2)_y & N_y \\ (X_1)_z & (X_2)_z & N_z \end{pmatrix} \begin{pmatrix} v_{j1} \\ v_{j2} \\ 0 \end{pmatrix}, \quad j = 1, 2 \quad (3.7)$$

In the variation process V_j , the $(X_1)_x$, $(X_1)_y$, etc. are the direction cosines of X_1 , X_2 and N in the global coordinate system, the v_{j1} and v_{j2} are coordinate of v_j in the local one[24].

3.1.2 Interpolation

Interpolation is a kind of mathematics method to get a list of unknown figures within some discrete set of know data. This method is always utilized in the case below(eq: 3.8), if we would to figure out the value of y_3 when x_3 equals three. The problems we

$$\begin{aligned} x_1 &= 1, y_1 = 2 \\ x_2 &= 2, y_2 = 3 \\ x_4 &= 4, y_4 = 5 \end{aligned} \quad (3.8)$$

meet are certainly more complex than the case above. There are a wide range of interpolation approaches to be selected depending on the problem domain, such as linear interpolation, polynomial interpolation, spline interpolation, etc.

In our research progress, the utilized interpolation approach is called inverse interpolation. In numerical analysis, inverse interpolation is a root-finding algorithm. For example, according the case above(eq:3.8), the normal interpolation is to figure out the value of y_3 when x_3 equals three, by contrast, the inverse interpolation is to calculate the value of x_3 when y_3 equals four.

$$\begin{aligned}
x_{n+1} = & \frac{f_{n-1}f_n}{(f_{n-2} - f_{n-1})(f_{n-2} - f_n)} x_{n-2} + \\
& \frac{f_{n-2}f_n}{(f_{n-1} - f_{n-2})(f_{n-1} - f_n)} x_{n-1} + \\
& \frac{f_{n-2}f_{n-1}}{(f_n - f_{n-2})(f_n - f_{n-1})} x_n
\end{aligned} \tag{3.9}$$

The definition of inverse interpolation is like the formula(3.9) above[25]. It is obvious that three initial value x_0 , x_1 and x_2 are necessitate in this method. Then, the Lagrange interpolation formula can be employed to conduct the quadratic interpolation on the inverse of f yields[26].

$$\begin{aligned}
f^{-1}(y) = & \frac{(y - f_{n-1})(y - f_n)}{(f_{n-2} - f_{n-1})(f_{n-2} - f_n)} x_{n-2} + \\
& \frac{(y - f_{n-2})(y - f_n)}{(f_{n-1} - f_{n-2})(f_{n-1} - f_n)} x_{n-1} + \\
& \frac{(y - f_{n-2})(y - f_{n-1})}{(f_n - f_{n-2})(f_n - f_{n-1})} x_n
\end{aligned} \tag{3.10}$$

3.1.3 Euclidean Distance

In two-dimensional environment, there are two points A and B and their coordinates are (x_1, y_1) and (x_2, y_2) , respectively(Fig. 3.3). As shown in the figure, there is a triangle made up by a solid line and two dashed lines. The length of two dashed lines are respectively the projection distance differences between the A and B in x-axis and in y-axis. This means the length of each of them is $y_2 - y_1$ and $x_2 - x_1$. Depending on the Pythagorean theorem, the length of solid line d (also denoted as $|\vec{AB}|$) is:

$$d = |\vec{AB}| = \sqrt{(y_2 - y_1)^2 + (x_2 - x_1)^2} \tag{3.11}$$

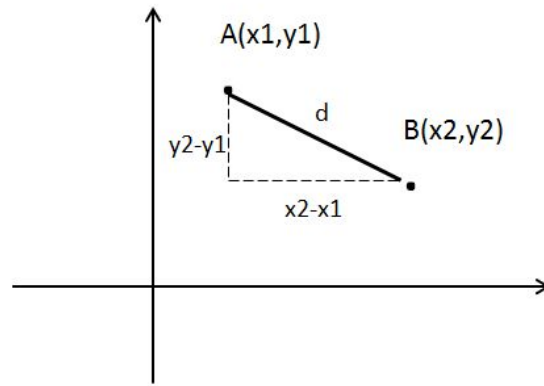


Figure 3.3: Euclidean Distance(2D)[6]

In three-dimensional environment, the length calculation of two point is similar with that two-dimensional case. Like the figure(Fig. 3.4), the coordinate of point P is (a, b, c) and point O is the origin. With utilizing Pythagorean theorem twice, the length of OP can be determined.

$$|\overrightarrow{PO}| = \sqrt{(a)^2 + (b)^2 + (c)^2} \quad (3.12)$$

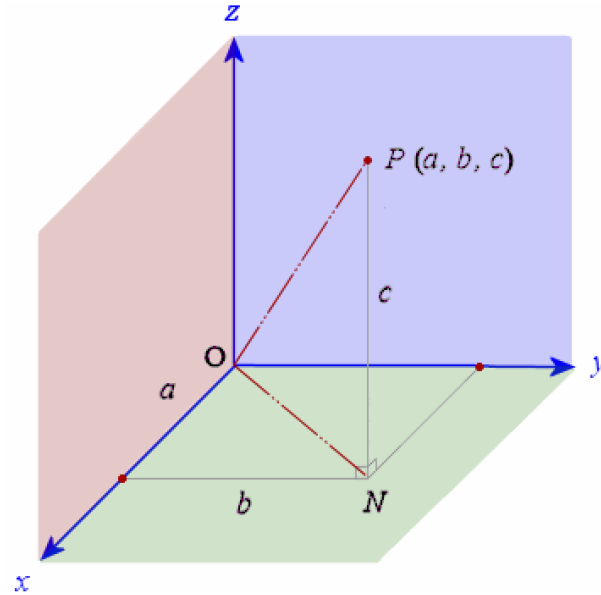


Figure 3.4: Euclidean Distance(3D)[7]

3.2 Analysis

The main mathematical concepts used in the development of the algorithm is divided into two parts: the calculation of principal curvature direction and the inverse interpolation. Then, the data will be handled by some particular software.

Previously, there were some approaches to model the aneurysm evolution. Compared with them, the new remodelling algorithm developed in this paper has some advantages and disadvantages as introduced below:

3.2.1 Improvements

- In some past researches, the remodelling progress was based on the standard model. By contrast, the algorithm developed in this paper achieves the remodelling progress by analysing the surface condition of aneurysm. It means that this algorithm is suitable for any aneurysm and fits the patient-specific demand.
- the algorithm developed in this paper utilizes the approach about anisotropic elasticity collagen remodelling, it will analyse not only the elastin degradation, but also the influence caused by collagen fibres reorientation, which will help to ensure the whole remodelling progress increasingly accurate.

3.2.2 Limitations

- In the preprocessing part, only the simplistic case was picked to conduct analysis.
- There are still some patient-specific aneurysm data needed to be confirmed, such as the value of shear modulus and etc.
- Due to the limitation of operational capability of personal computer, only 5 aneurysm growth times periods was modelled.

- Because the algorithm developed in this paper was implemented in four different programming languages, the UI part have not been designed. The compiler works in batch mode, it has no methods to prompt the user for data.

Chapter 4

Implementation

The aim of the entire system is to model the aneurysm evolution progress. This will help to obtain a better understanding of this disease. The program developed for the modelling is based on the four programming languages: Matlab [27], APDL [28], FORTRAN [29] and Perl [30].

4.1 The Prepare of Modelling Aneurysm Evolution

In this part, we should create the basic aneurysm model by meshing and analysing the surface of aneurysm. The process is like the flow chart(4.1) below:

4.1.1 The Establishment of the Aneurysm Model

The establishment of the aneurysm model is mainly about meshing. It means that the surface of aneurysm will be divided into a wide range of grids(elements). It is important to build several proper grids because these grids will affect the final remodelling of aneurysm. The more grids we build, the more specific the overall model will be. However, the disadvantage is that the corresponding calculation will

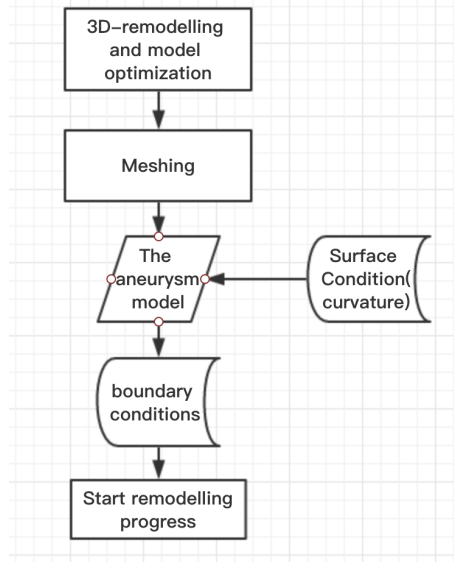


Figure 4.1: Preprocessing Part of Remodelling

be more complex. Hence, in the meshing part, not only the quality of grids(elements) should be controlled, but also the number of grids should be paid attention to.

In this case, because aneurysm is a kind of irregular geometry, it is difficult to build a series of structured grids. In terms of its uneven surface, in order to ensure the computational accuracy, there are two meshing strategies: hexahedron elements and tetrahedron elements. Both of them have their own advantages. Because one hexahedron element only has 8 nodes, it can obviously reduce the following calculating difficulty. However, due to the structure of hexahedron, a complicated model is hard to be meshed only by several hexahedron elements. Turning to tetrahedron meshing approach, by contrast, it can be easily used to mesh. In addition, standard tetrahedron(Fig. 4.2) only has four vertexes. If only the standard tetrahedron used, the whole model will not be precise with the limitation of calculation points. Hence, in this paper, the tetrahedrons with intermediate points(Fig. 4.2) are utilized because it has 10 nodes, which will conspicuously improve the computational accuracy.

By tetrahedrons with 10 nodes, the aneurysm can be meshed in three-dimensional environment like the figure(Fig. 4.3) below. In this aneurysm model, there are 67325 nodes and 34134 elements(tetrahedrons). The next step is to analyse its surface geometry.

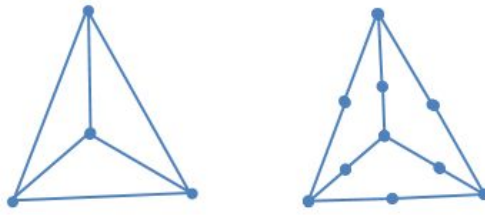


Figure 4.2: Standard Tetrahedron and Tetrahedron with Intermediate Points

4.1.2 Analysis of Principal Curvature of Aneurysm Geometry

In this part, the surface geometry of aneurysm should be analysed. In order to ensure the validity of remodelling progress, a new aneurysm model, which is between the inner surface of aneurysm and outer surface, is created. The surface geometry of this new model is achieved by the inverse interpolation approach, which interpolates the first and second principal curvature directions from inner and outer surface into the new aneurysm model.

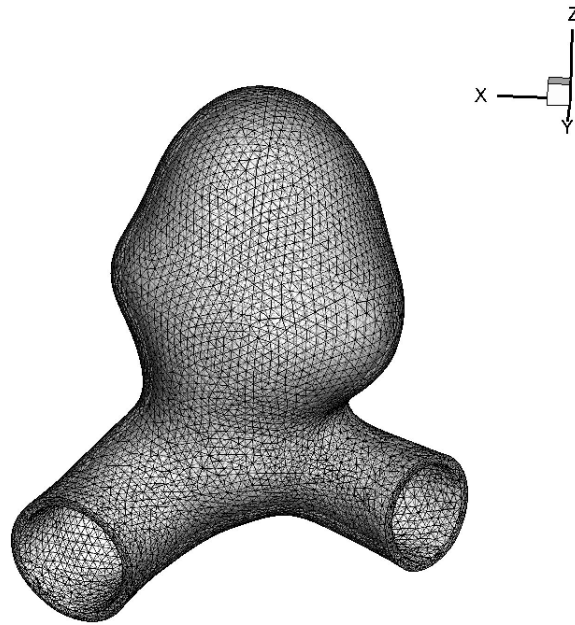


Figure 4.3: The Meshing Result

The calculations of first and second principal direction about inner and outer surface of aneurysm are the same, hence, the description will be combined. Utilizing the approach introduced in the Chapter 3, the principal directions can be achieved. Then, the software 'Tecplot360' is operated to conduct the inverse interpolation. The reason why we choose this software is that the interpolation algorithm was integrated into this software, the only thing we should do is to write a data file with the standard commander header. This will considerably decrease the complexity of the whole application. And, more remarkable, after interpolation, the output data file still require normalization. Hence, there are two final data files: the first and the second principal directions of elements of the new aneurysm model.

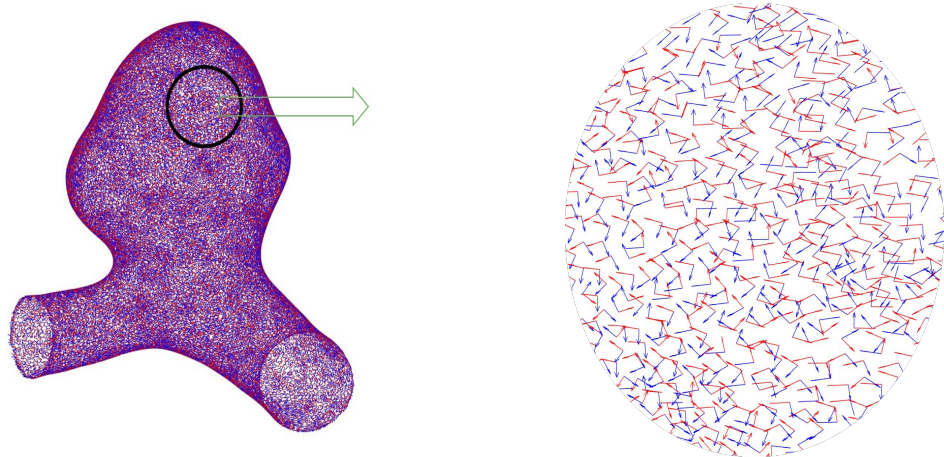


Figure 4.4: The Distribution of Principal Curvature(1st and 2nd) Direction of new Aneurysm model. (In addition, the red vector is the 1st principal direction and the blue vector is the 2nd principal direction)

4.1.3 Determination of the Initial Parameters

As mentioned above, the Holzapfel's model is applied to conduct the anisotropic elasticity collagen remodelling. In order to compare the initial aneurysm model with the grown-up one, the original condition should be determined. Due to the formula explanation in 'Ansys'[8], the exponential-function-based strain energy potential is

given by:

$$W_d(C, A \otimes A, B \otimes B) = \sum_{i=1}^3 a_i(\bar{I}_1 - 3)^i + \sum_{j=1}^3 b_j(\bar{I}_2 - 3)^j + \frac{c_1}{2c_2} \{ \exp[c_2(\bar{I}_4 - 1)^2] - 1 \} + \frac{e_1}{2e_2} \{ \exp[e_2(\bar{I}_6 - 1)^2] - 1 \} \quad (4.1)$$

In this case, we only pay attend to the variation of I_1 , I_4 and I_6 . Also, in order to reduce calculation amount, the value of c is set to equal with that of e . It means that, the strain energy function is the same with what we have introduced in Chapter 2.

TBOPT	Constants	Purpose	Input Format
POLY	C1 to C31	Anisotropic strain energy potential	TB,AHYPER,,,POLY TBDDATA,,A1,A2,A3,B1,...
EXP	C1 to C10	Exponential anisotropic strain energy potential	TB,AHYPER,,,EXPO TBDDATA,,A1,A2,A3,B1,B2,B3 TBDDATA,,C1,C2,E1,E2
AVEC	C1 to C3	Material direction constants	TB,AHYPER,,,AVEC TBDDATA,,A1,A2,A3
BVEC	C1 to C3	Material direction constants	TB,AHYPER,,,BVEC TBDDATA,,B1,B2,B3
PVOL	C1	Volumetric potential	TB,AHYPER,,,PVOL TBDDATA,,D

Figure 4.5: Ansys Input Format[8]

According to the description about the exponential-function-based strain energy potential(Fig. 4.5), the key word "PVOL" represents the volumetric potential and its value D equals $1/k$ [8], where k is the bulk modulus. As Mohammed Yahya[31] denoted, the value of initial bulk modulus k is 34.7 MPa . Consequently, the volumetric potential have been determined. Note that, for lack of supporting of relevant paper information, the definition of the initial parameters k_2 and c are determined by ourselves, 40 and 0.8, respectively.

4.1.4 The Boundary Condition

In the finite element calculation, boundary condition is a significant part. Only with these boundary conditions, the solution of equation will have its own arithmetical mean and geometric mean. In this case, because the environment of aneurysm

evolution is influenced by blood flow, the pressure elected is the same as blood pressure: $120mmHg$. On top of that, the aneurysm utilized in this case includes a portion of artery. Given that the aim of the research is to model the aneurysm evolution, this extra artery should be fixed. It means that in the growth progress, the displacement of artery must equal zero.

4.2 The Modelling Loop of the Growth Process of Aneurysm

This part is the implement of the modelling the aneurysm growth. Considering that three softwares are operated, The programming language "Perl"[30] is promoted to control the whole progress. We can easily write some shell codes by calling the 'system' command to execute some user scripts. This will help us to link the three softwares together and achieve the automation goal.

4.2.1 Overview of Whole Progress

In general, the whole process is a loop of assigning each element their own material parameters and calculating the remodelling results by computing the above function (eq:4.1), which can be represent as the flow chart below:

Note that, among the parameter list, the value of k_2 will be affected by the previous remodelling result. Meanwhile, the value of shear modulus(c) will stably decrease by the time interval.

4.2.2 Handling the Parameter by Utilizing Holzapfel Model

Following the strategy (eq:4.1) mentioned above, for each remodelling loop, we should create the corresponding data file. In other words, if users would like to

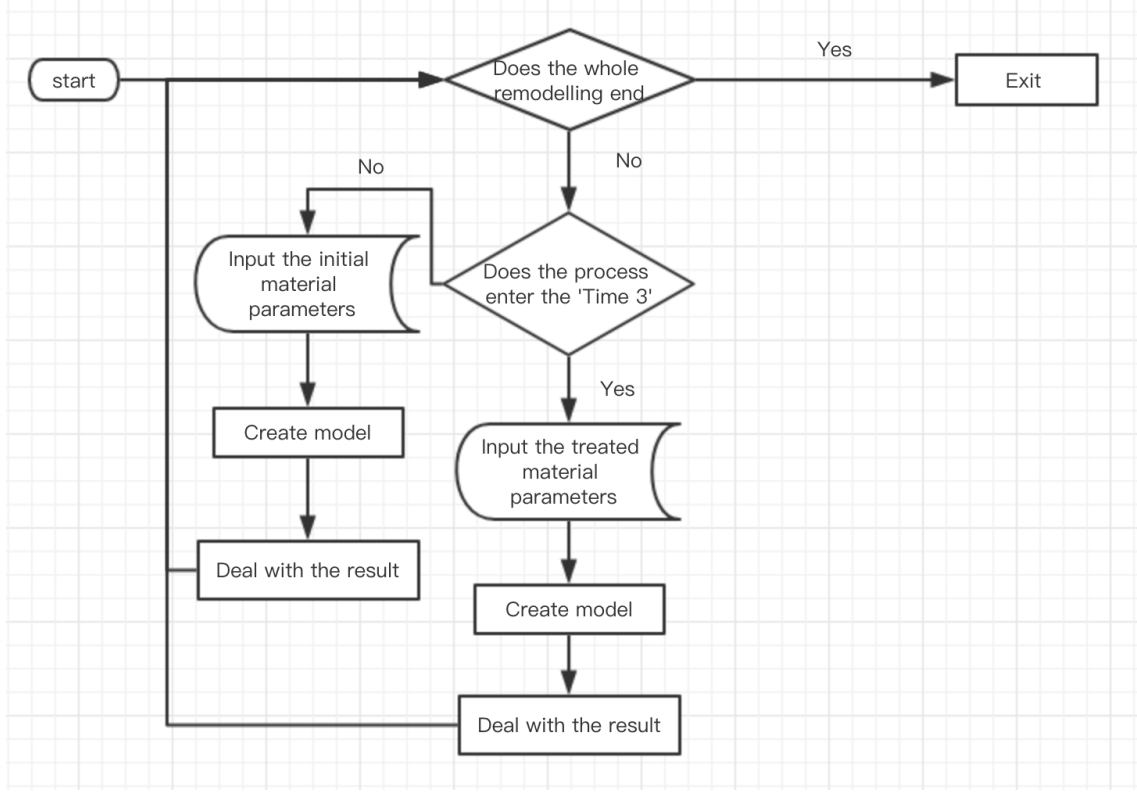


Figure 4.6: The Flow Chart of Remodelling Progress

model growth processes of four time intervals, there will be four data files about the material parameters of each element. In each data file creating procedure, we must absolutely follow the input format (denoted in Fig. 4.5) provided by 'Ansys'[28].

The first and second remodelling process is the initial condition. In this two special remodelling process, the values of c are set as 0.8 and 0.7. The decrease rate (0.1) is different from the after figures, which will be 0.13. In addition, from the 'Time 3' to later time interval, the material parameters (mainly k_2) demand to be settled by comparing the result of 'Time 1' with that of the previous time interval. Furthermore, the time complexity will increase in a linear trend with the boost of remodelling time periods. For example, when the 'Time 2' is remodelled, the 'Anasys '[28] will not only calculate the expansion of the aneurysm in 'Time 2', but also calculate the result of 'Time 1' and apply this as the foundation model of the 'Time 2' process. A huge amount of arithmetic capability is required if we would like to remodel a relative late time interval.

4.2.3 The Algorithm to Deal With the Output Stress Results

In each of the third time interval and late ones, in order to acquire the value of k_2 , the corresponding output stress results should be handled by a special Algorithm. There is a hypothesis equation defined by:

$$\frac{\partial k_2}{\partial t} = -\tau \left(\frac{\sigma g - \sigma h}{\sigma h} \right) k_2 \quad (4.2)$$

where g represents the stress value of k_2 of the latest model, h represents the stress value of k_2 of the first model and τ is the symbol of collagen growth rate. This equation (eq: 4.2) demonstrates the rate of change of k_2 . The recent value of k_2 is achieved by adding original value and this variation. Similarly, the value of collagen growth rate (0.8) is determined by ourself.

With this hypothesis equation, what we should do is to extract the stress parameters from the two particular model status. Among all produced data matrix, the value of S_1 is helpful for us because the absolute value of S_1 is the maximum component and can reflect bearing condition of one specific fiber element best. However, due to the format limitation of produced data file, not only the S_1 is extracted, but also some other information. Furthermore, the S_1 is attached on each node. It means that we also need to conduct the data transformation from 'node' to 'element'. Corresponding to each element, the value of S_1 can be achieved.

As mentioned above, the whole aneurysm geometry is meshed by a wide range of tetrahedrons. It means that one element is consist of four nodes information. These four node S_1 are just averaged to get the element S_1 , which should be improved if there is a better solution in the future.

4.2.4 Region Control

By employing approaches above, the whole aneurysm geometry evolution can be realized. Turning to the particular geometry evolution, the framework is similar.

In order to realize the localization modelling, the value of material parameters of related element should be different from that of other element. It means that the value of material parameters of those element in the specific domain should be modified manually. The material parameter should be changed is the value of shear modulus (c), which should be set lower than the adjoining region. The algorithm used here is to divided the whole aneurysm model (4.8) into three parts by the value of shear modulus.

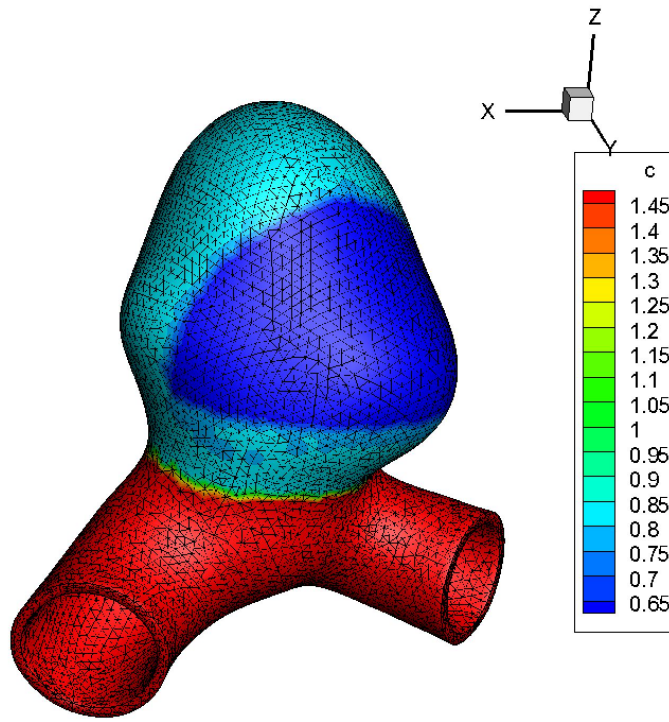


Figure 4.7: The Distribution of Different Value of the Related Material Oarameters(c) in the Aneurysm Model

The below part of the aneurysm model is the artery part. The blue area is the selected localization modelling domain. In order to observe the obvious change of this particular area. All changes of material parameters just happens in this area. It means that the value of shear modulus in this area will reduce while the value of shear modulus in other place will keep the same as the initial value (Fig. 4.8). This can control that the growth and remodelling only occurs in the the selected domain.

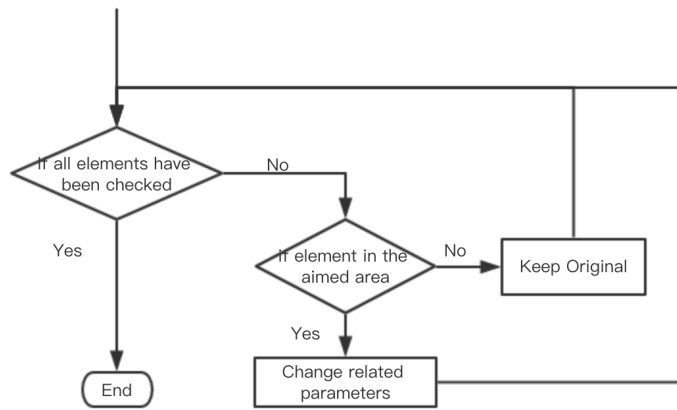


Figure 4.8: The Process of How the Related Material Parameters Change

The next step is to determine how to mark off this special area. There are two special element picked out first. One is the center point of the whole aimed localization modelling realm and the other is the ragged edge of the realm. There is a circle, its dot is the first point and radius is the distance between these two points. Although, this circle will be transferred into a irregular graph if this is 3D-projected on the aneurysm model.

Chapter 5

Results and Discussions

5.1 The Results about Pintcipal Curvature Direction of Different Aneurysms

On the basis of the algorithm introduced in the above chapter, the distribution of principal curvature (1st and 2nd) direction of the aneurysm's surface geometry can be confirmed. Three patient-specific aneurysms are handled, and figures below(5.1,5.2 and 5.3) demonstrate their own conditions.

In consideration of the structure of artery, in order to fit the patient-specific demand better, the target aneurysm will be divided into two parts: inner and outer surface. These two parts will be analysed for the next research step, respectively.

5.2 Data Processing Progress

After obtaining the surface information of aneurysm, the interpolation and normalization should be finished to process data further. The following step is to a remodelling loop according to the growing time. In each remodelling progress, the values of

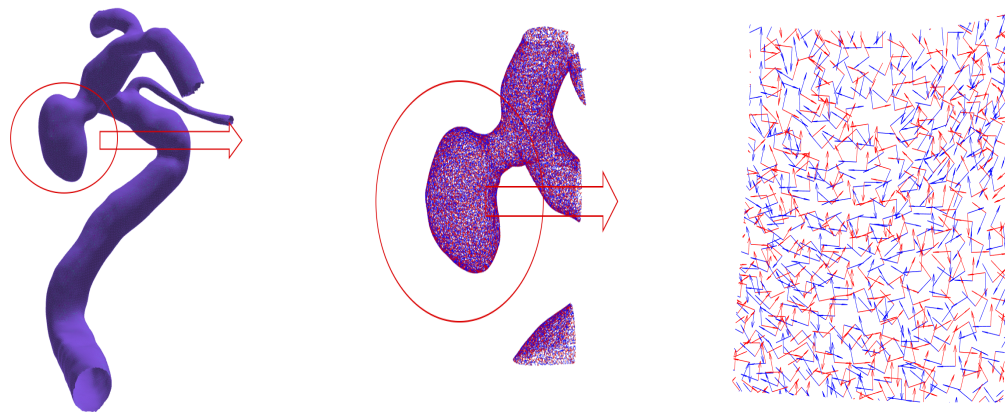


Figure 5.1: The Distribution of Principal Curvature(1st and 2nd) Direction of Aneurysm(1)

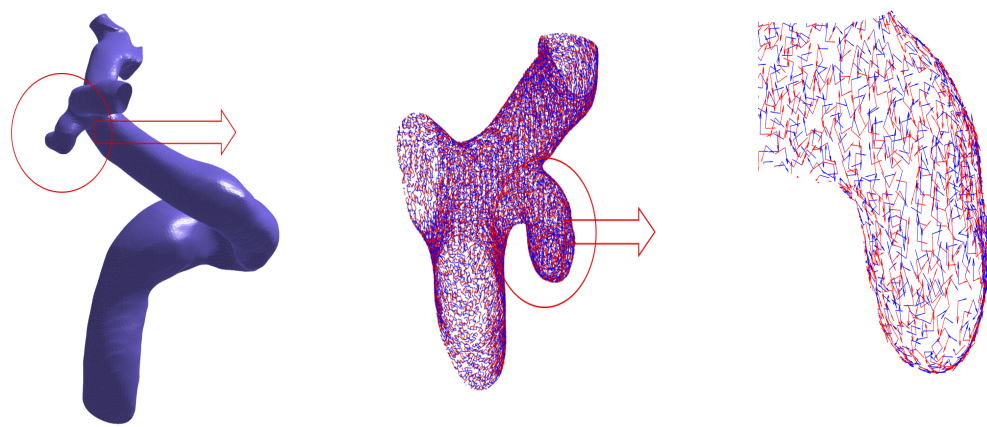


Figure 5.2: The Distribution of Principal Curvature(1st and 2nd) Direction of Aneurysm(2)

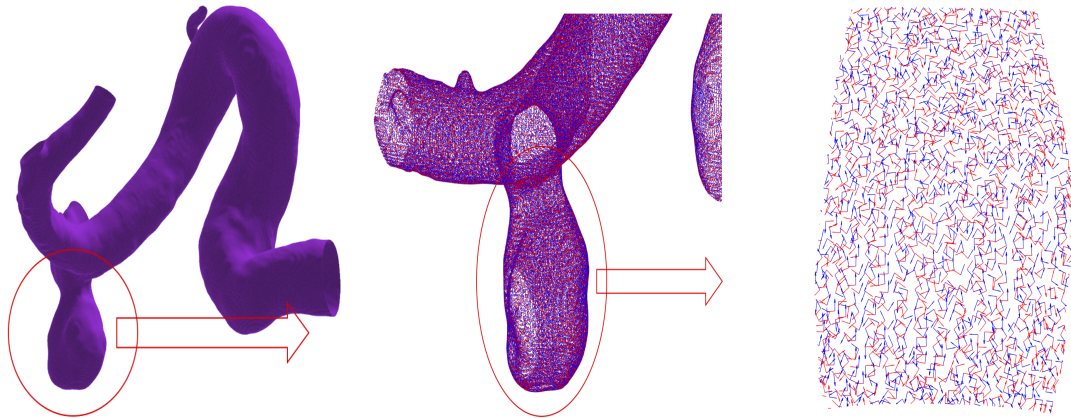


Figure 5.3: The Distribution of Principal Curvature(1st and 2nd) Direction of Aneurysm(3)

some material parameters, including shear modulus, bulk modulus, k_2 and material directions, are supposed to be setted. The following flow chart (5.4) illustrates the whole progress.

This flow chart (Fig.5.4) is for the remodelling progress of the whole aneurysm geometry. In terms of the input material parameters, the directions of fiber orientation and the value of bulk modulus are fixed. The rate of shear modulus decrease by time period and k_2 is influenced by the the first principal stress created by remodelling model in the last step.

5.3 The Modelling of Aneurysm Evolution about Whole Geometry

There is a table(Table 5.1) to demonstrate the growing rate of each time period. c and k_2 represent shear modulus, exponential anisotropic strain energy potential parameter, respectively. DMX is the simplified form of 'Displacement Max', which is the longest distance of a particular element shifts. It is used to explain how much the aneurysm model has grown. In addition, there are four figures (Fig. 5.5) to illustrate the remodelling circumstance of each element.

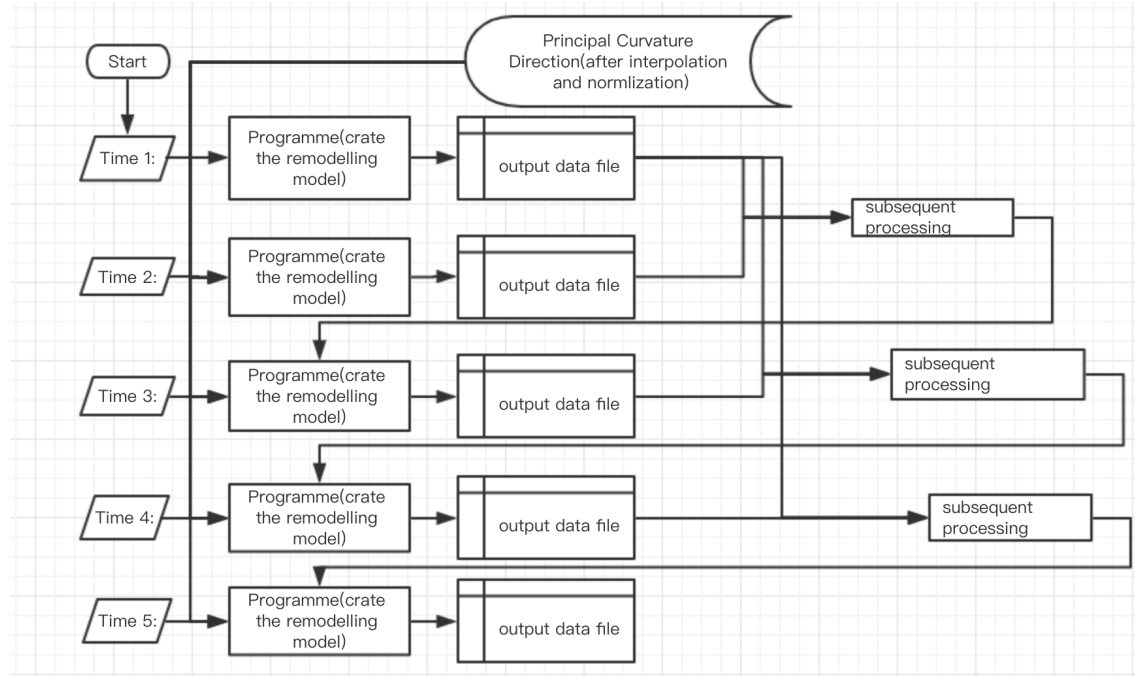


Figure 5.4: The Flow Chart of Remodelling Progress

	Time 1	Time 2	Time 3	Time 4	Time 5
The value of c	0.8	0.7	0.57	0.44	0.31
The value of k_2	40	40	change by Time	change by Time	change by Time
The value of DMX	0.293608	0.326683	0.385691	0.477779	0.647269

Table 5.1: The DMX in Different Parameters

Among the modelling figures (Fig. 5.5), the regions with more red in color has more element displacement and it means there is higher growth rate for fibers in these regions. Compared with the initial status 'Time 1' (Fig. 5.6(a)), the aneurysm evolution is not so obvious in 'Time 2' (Fig. 5.6(b)). By contrast, there is a clear darken process ,which also represents the aneurysm growth, in 'Time 3' (Fig. 5.6(c)) and 'Time 5' (Fig. 5.6(d))).

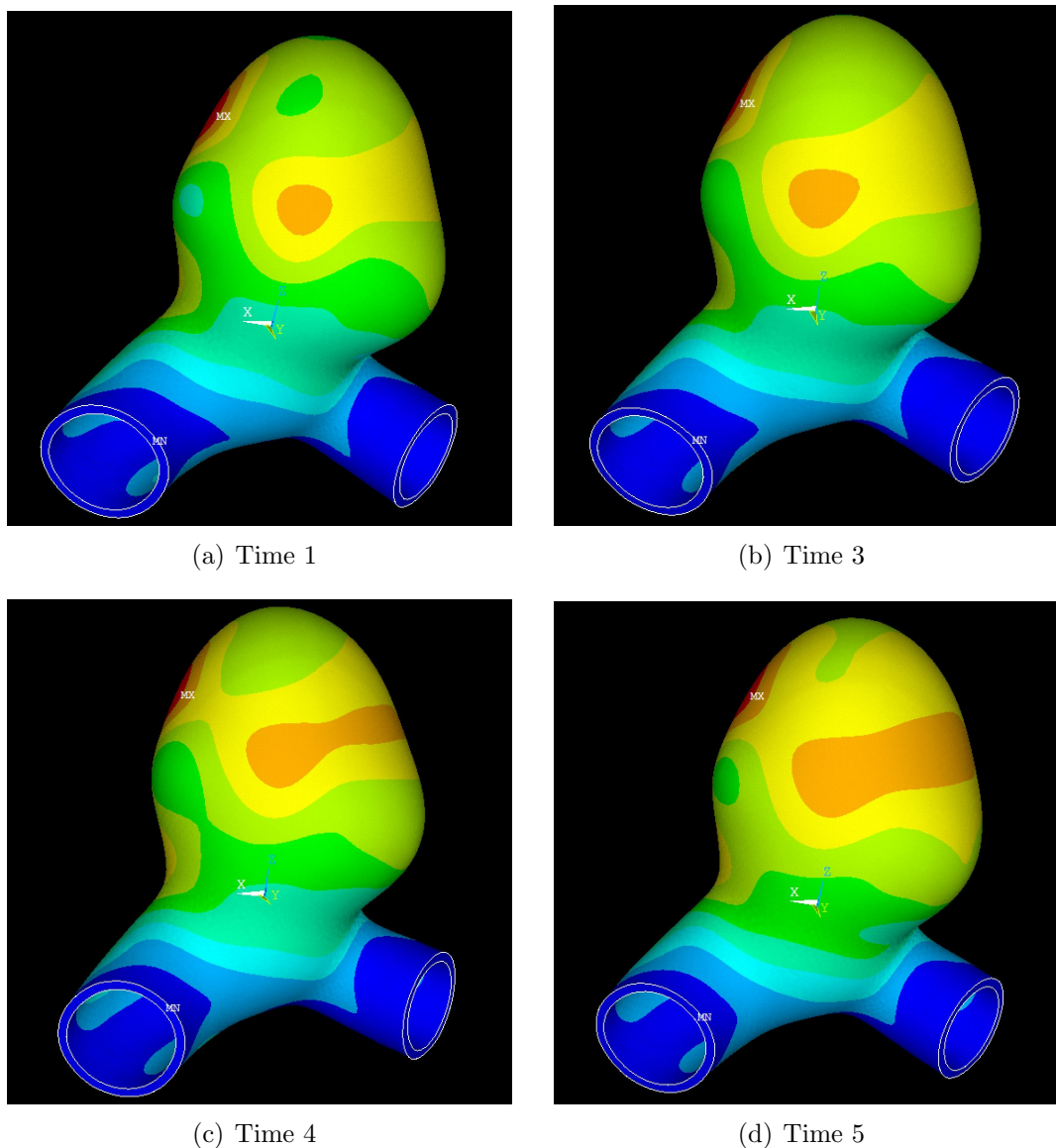


Figure 5.5: Modelling of Aneurysm Whole Geometry Evolution

5.4 The Modelling of Aneurysm Evolution about the Localization Part

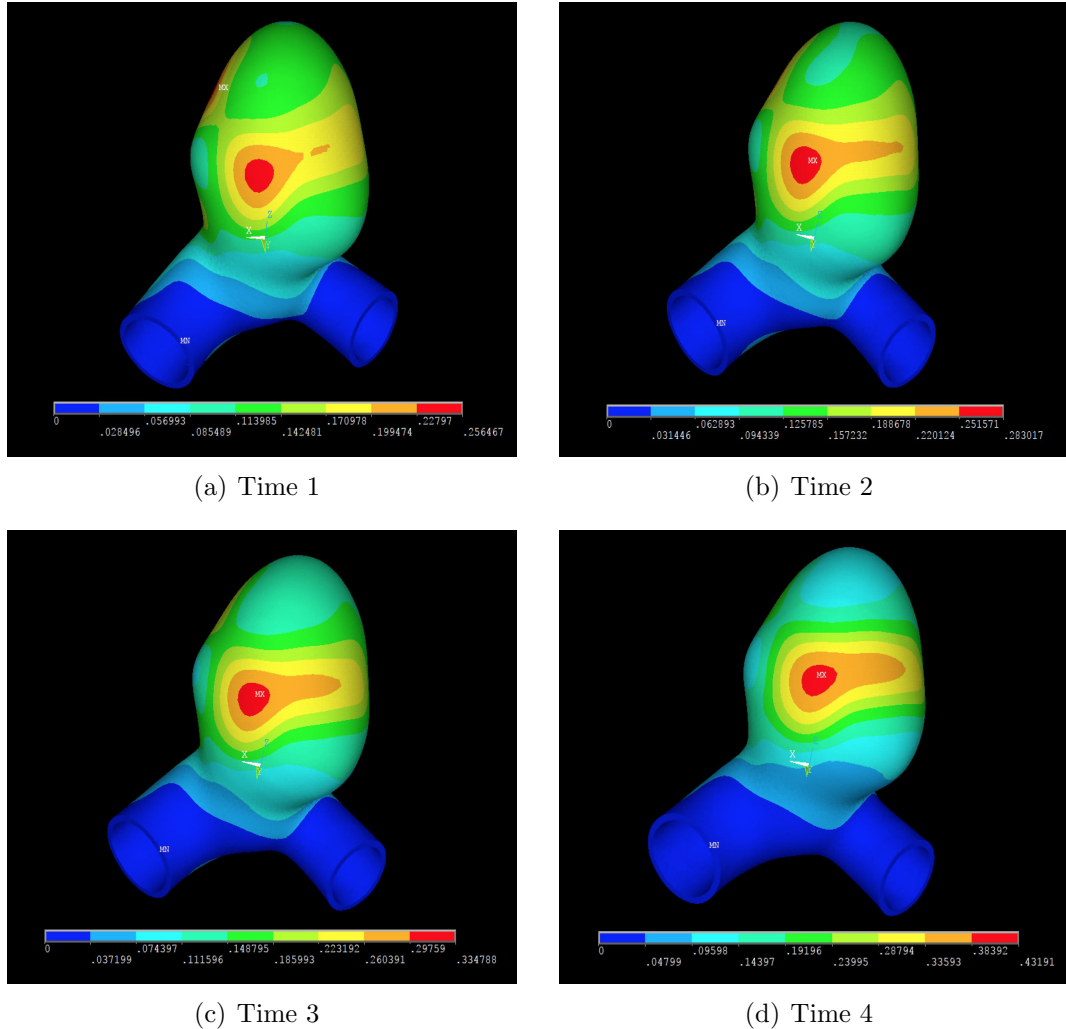


Figure 5.6: Modelling of Aneurysm Localization Evolution

The modelling of aneurysm evolution about the particular domain can be achieved by adjusting the material parameters of the elements in this area. The values of c are kept as 1.5 in the artery part and 0.8 in the no-e-selected area, respectively. In terms of the localization domain, the changes of shear modulus will be displayed in the table below:

	Time 1	Time 2	Time 3	Time 4
The value of c	0.67	0.57	0.44	0.31
The value of DMX	0.256467	0.283017	0.334788	0.43191

Table 5.2: The Change of Shear Modulus (c) of the Localization Domain

This modelling process is similar with that of whole geometry of aneurysm. There are four time periods (Fig. 5.6) which have been remodelled. Note that, although it is shown that a obvious layered color pattern in the center of each figures, these colors represent their own values. There is a color map bar at the bottom of each time period figures. It is illustrated that in the selected area, a growth process can be detected. The maximum of element displacement raises from 0.256467 in 'Time 1' to 0.43191 in 'Time 4'. In other part of this aneurysm model, the each element displacement almost remains the same as that of 'Time 1'.

Chapter 6

Conclusion

6.1 Conclusion

During two months period of this project, different technologies have been studied. The greatest achievement of this project is that it is successful to develop the modelling of intracranial aneurysm evolution by analysing the surface geometry of aneurysm. This can be used further in some related applications. Overall, this project can be divided into two parts about the modelling creating algorithm and the growth process modelling algorithm.

With utilizing tetrahedron with intermediate points, the initial meshing algorithm of the aneurysm model was successfully implemented. Turning to the analysis of the surface geometry of aneurysm, some difficulties about calculating algorithm were detected because of the limitation of some related curvature mathematics foundation. The whole problems were addressed by importing the curvature calculating algorithm [32] created by Itzik Ben Shabat. The calculating process operated as a "black box". This algorithm was initially tested on standard 'peak' hook face and result was compared to check its accuracy, after which it was applied to the reconstructed complex aneurysm surface geometry meshed before. On obtaining the principal directions required, the main part of analyse the aneurysm surface geometry was completed. However, the final surface result demanded should be achieved by normalizing the data obtained by the curvature algorithm, this will

reduce the chances of any aberration.

In order to round off the project, the "ANSYS" software [28] was utilized to modelling the aneurysm evolution. After giving each surface element their own material parameters, this software will present an insight about the patterns of different remodelling period, including various related parameters, such as Stress, DMX, etc, which are important in the next modelling step. The above remodelling process is supposed to be repeated by some certain loop control codes to acquire the whole modelling of the aneurysm evolution.

6.2 Limitations

Though that some modelling results can be achieved, there are still some limitations about this model, which are listed below:

- The most important disadvantages of this model is the determination of the value of related input material parameters. There are some material parameters without the supporting of previous papers, such as the shear modulus about the aneurysm. In addition, the equation connecting the value of stress and k_2 should be studied further.
- The algorithm only detects a standard aneurysm model. More patient-specific aneurysm should be tested to obtain their evolution results.
- The whole model only concerns the influence made by the blood environment. It means that all material parameters are associated with the change of blood environment. However, in reality, the remodelling of aneurysm will in return affect the hemodynamic environment. In this model, this phenomenon has not been taken into consideration.

Chapter 7

Future Work

It is just beginning of possible prospects in the future about the final result producing the modelling of patient-specific aneurysm evolution. A large number of applications are possible with this project as the basis.

Linking with the Blood Environment

The model will more accurate if the influence made by the aneurysm evolution to the hemodynamic environment can be linked with. In other words, the future work is to connect the model with "fluid".

It has been proved that this can work. In the paper of professor Paul Watton [14], there are some information can be used to support. Wall shear stress (WSS) is the most important parameter about the arterial wall deformation due to the blood flow. It has been known that high values of wall shear stress is associated with the growth of aneurysm. The high wall shear stress is able to lead to the formation of an aneurysm and the low wall shear stress is linked with the aneurysm evolution. There is a equation that can demonstrate the relationship between the wall shear stress and the degradation of elastin.

$$\frac{\partial m^E}{\partial t} = -F_D(\tau(\theta_1, \theta_2, t))D_{max}m^E(\theta_1, \theta_2, t) \quad (7.1)$$

F_D is a function (below) about the relationship between WSS and the degree of the degradation of elastin.

$$F_D(\tau((\theta_1, \theta_2, t))) = \begin{cases} 0, & \tau \geq \tau_{Crit} \\ (\frac{\tau_{Crit}-\tau}{\tau_{Crit}-\tau_X})^2, & \tau_{Crit} > \tau > \tau_X \\ 1, & \tau > \tau_X \end{cases} \quad (7.2)$$

In the equation[14] above, τ_{Crit} means the maximum value of the WSS during the cardiac cycle is greater than a critical value and there is no degradation of elastin occurs. Turning to τ_X , it is an existing value between 0 and τ_{Crit} and in this value, the maximum degradation of elastin occurs[14].

When $F_D = 0$ (WSS over a critical value), it means that no degradation progress occurs, nevertheless, when $F_D = 1$ (WSS equals below a critical minimum value), it means that the maximum degree of degradation occurs[15].

Problems about the Calculation of k_2

As mentioned before, this is a hypothesis about the related equation and parameters. This algorithm would be improved by an alternative formula.

The Data Structure

In the process of setting the initial parameters and the decreasing gradient of shear modulus (c), all data must be changed in the particular "matlab" codes. In the future work, a special data should be created and all parameters should be changed and saved in this file. Then, total associative programs must take data from this file. If it works, it will not only improve user experience, but reduce the possibility that user modify codes mistakenly as well.

Other Fields of Study

It is a considerably large to combine different disciplines knowledge, such as mathematics, computer science and biomechanics, together and apply to this project.

Maybe, there are some of the concepts like the aneurysm meshing can be more effectively. Overall, it would be applicable for the primary propose of the ideas presented in a global perspective.

Bibliography

- [1] J. L. Brisman, J. K. Song, and D. W. Newell, “Cerebral Aneurysms,” *Nejm*, vol. 355, no. 9, pp. 928–939, 2006.
- [2] J. C. Lasheras, “The Biomechanics of Arterial Aneurysms,” *Annual Review of Fluid Mechanics*, vol. 39, no. 1, pp. 293–319, 2007.
- [3] K. M. Naseem, “The role of nitric oxide in cardiovascular diseases,” *Molecular Aspects of Medicine*, vol. 26, no. 1-2 SPEC. ISS., pp. 33–65, 2005.
- [4] E. Gaba, “View of the planes establishing the main curvatures on a minimal surface.” https://commons.wikimedia.org/wiki/File:Minimal_surface_curvature_planes-en.svg.
- [5] the lonely wolf, “Local orthogonal coordinate system.” <http://www.92to.com/shehui/2016/05-19/4755631.html>.
- [6] L. Yu, “The deep learning.” <http://www.cnblogs.com/yulinfeng/p/4508930.html>.
- [7] “The 3-dimensional co-ordinate system.” <https://www.intmath.com/vectors/6-3-dimensional-space.php>.
- [8] APDL, “Apdl help documents–hyperelasticity.” https://www.sharcnet.ca/Software/Ansys/16.2.3/en-us/help/ans_mat/aQw8sq22dldm.html.
- [9] B. Kim, S. B. Lee, J. Lee, S. Cho, H. Park, S. Yeom, and S. H. Park, “A comparison among Neo-Hookean model, Mooney-Rivlin model, and Ogden model for Chloroprene rubber,” *International Journal of Precision Engineering and Manufacturing*, vol. 13, no. 5, pp. 759–764, 2012.

- [10] G. A. Holzapfel, T. C. Gasser, and R. Ogden, “A new constitutive framework for arterial wall mechanics and a comparative study of material models,” *Journal of elasticity*, vol. 61, no. 1, pp. 1–48, 2000.
- [11] G. A. Holzapfel, T. C. Gasser, and M. Stadler, “A structural model for the viscoelastic behavior of arterial walls: continuum formulation and finite element analysis,” *European Journal of Mechanics-A/Solids*, vol. 21, no. 3, pp. 441–463, 2002.
- [12] S. Avril, P. Badel, and A. Duprey, “Anisotropic and hyperelastic identification of in vitro human arteries from full-field optical measurements,” *Journal of biomechanics*, vol. 43, no. 15, pp. 2978–2985, 2010.
- [13] S. Zhao, X. Xu, A. Hughes, S. Thom, A. Stanton, B. Ariff, and Q. Long, “Blood flow and vessel mechanics in a physiologically realistic model of a human carotid arterial bifurcation,” *Journal of biomechanics*, vol. 33, no. 8, pp. 975–984, 2000.
- [14] P. N. Watton, A. Selimovic, N. B. Raberger, P. Huang, G. A. Holzapfel, and Y. Ventikos, “Modelling evolution and the evolving mechanical environment of saccular cerebral aneurysms,” *Biomechanics and Modeling in Mechanobiology*, vol. 10, no. 1, pp. 109–132, 2011.
- [15] A. Selimovic, Y. Ventikos, and P. N. Watton, “Modelling the evolution of cerebral aneurysms: Biomechanics, mechanobiology and multiscale modelling,” *Procedia IUTAM*, vol. 10, pp. 396–409, 2013.
- [16] R. L. Satcher and C. F. Dewey, “Theoretical estimates of mechanical properties of the endothelial cell cytoskeleton,” *Biophysical journal*, vol. 71, no. 1, pp. 109–18, 1996.
- [17] K. Takamizawa and K. Hayashi, “Strain energy density function and uniform strain hypothesis for arterial mechanics,” *Journal of biomechanics*, vol. 20, no. 1, pp. 7–17, 1987.
- [18] P. Boulanger and M. Hayes, “Finite-amplitude waves in mooney-rivlin and hadamard materials,” in *Topics in finite elasticity*, pp. 131–167, Springer, 2001.
- [19] M. R. Roach and A. C. Burton, “The reason for the shape of the distensibility curves of arteries,” *Canadian journal of biochemistry and physiology*, vol. 35, no. 8, pp. 681–690, 1957.

- [20] B. Ma, J. Lu, R. E. Harbaugh, and M. L. Raghavan, “Nonlinear anisotropic stress analysis of anatomically realistic cerebral aneurysms,” *Journal of biomechanical engineering*, vol. 129, no. 1, pp. 88–96, 2007.
- [21] W. Carver, M. L. Nagpal, M. Nachtigal, T. K. Borg, and L. Terracio, “Collagen expression in mechanically stimulated cardiac fibroblasts.,” *Circulation research*, vol. 69, no. 1, pp. 116–122, 1991.
- [22] Wikipedia, “Principal curvature.” https://en.wikipedia.org/wiki/Principal_curvature.
- [23] M. Spivak, “comprehensive introduction to differential geometry. vol. iv.[a],” 1981.
- [24] B. Ma, R. E. Harbaugh, and M. L. Raghavan, “Three-dimensional geometrical characterization of cerebral aneurysms,” *Annals of biomedical engineering*, vol. 32, no. 2, pp. 264–273, 2004.
- [25] J. F. Epperson, *An introduction to numerical methods and analysis*. John Wiley & Sons, 2013.
- [26] Wikipedia, “Inverse quadratic interpolation.” https://en.wikipedia.org/wiki/Inverse_quadratic_interpolation.
- [27] Matlab, “The introduction of matlab.” <https://uk.mathworks.com/products/matlab.html>.
- [28] Ansys, “The introduction of ansys-apdl.” <http://www.ansys.com/en-GB/Services/training-center/structures/introduction-to-ansys-mechanical-apdl>.
- [29] Tecplot360, “The introduction of tecplot360-fortran.” <http://www.tecplot.com/products/tecplot-360/>.
- [30] Perl, “The introduction of perl.” <https://www.perl.org/>.
- [31] M. Yahya, “Three dimensional finite-element modeling of blood flow in elastic vessels : effects of arterial geometry and elasticity on aneurysm growth and rupture VESSELS : EFFECTS OF ARTERIAL,” , 2010.

- [32] I. B. Shabat, “Curvature estimationl on triangle mesh.”
[https://uk.mathworks.com/matlabcentral/fileexchange/
47134-curvature-estimationl-on-triangle-mesh.](https://uk.mathworks.com/matlabcentral/fileexchange/47134-curvature-estimationl-on-triangle-mesh)